

## Thermal stabilization of the hcp phase in titanium

Sven P. Rudin,<sup>1</sup> M. D. Jones,<sup>2</sup> and R. C. Albers<sup>1</sup><sup>1</sup>*Los Alamos National Laboratory, Los Alamos, New Mexico 87545, USA*<sup>2</sup>*Department of Physics and Center for Computational Research, University at Buffalo, The State University of New York, Buffalo, New York 14260, USA*

(Received 14 October 2003; published 30 March 2004)

We have used a tight-binding model that is fit to first-principles electronic-structure calculations for titanium to calculate quasiharmonic phonons and the Gibbs free energy of the hexagonal-close-packed (hcp) and omega ( $\omega$ ) crystal structures. The hcp phonon dispersion agrees with experiment; the  $\omega$  phonon dispersion has yet to be measured. The model predicts that the true zero-temperature ground state is the  $\omega$  structure and that it is the entropy from the thermal population of phonon states which stabilizes the hcp structure at room temperature. We present a completely theoretical prediction of the temperature and pressure dependence of the hcp- $\omega$  phase transformation and show that it is in good agreement with experiment. The quasiharmonic approximation fails to adequately treat the bcc phase because the calculated phonons of this structure are not all stable.

DOI: 10.1103/PhysRevB.69.094117

PACS number(s): 64.30.+t, 63.20.Dj, 64.70.Kb, 65.40.Gr

The experimentally observed equilibrium state of titanium at room temperature is the hexagonal-close-packed (hcp) structure,<sup>1</sup> even though static-lattice first-principles electronic-structure calculations<sup>2-6</sup> predict the omega ( $\omega$ ) structure to be the energetically favored ground state. There are two possible causes for this discrepancy: (1) this is another failure of the first-principles methods (local-density approximation or generalized gradient approximation to density-functional theory) used for calculating the electronic-structure of solids, or (2) thermal effects stabilize the hcp phase. In this paper we show evidence that supports the second argument being correct: the thermal occupation of phonon states favors the hcp structure above a pressure-dependent transition temperature. Only by including the vibrational entropy in the first-principles calculations can theory be brought into agreement with experiment.

Titanium is a good case for testing our ability to predict solid-solid phase transformations with first-principles methods. It is an element that displays a rich phase diagram with several recently discovered high-pressure phases.<sup>7,8</sup> When alloyed with other elements, it leads to materials of major technical importance for the airline, space, and other industries.

Extensive experimental studies of the pressure-induced transition from the hcp to the  $\omega$  structure at room temperature show a large hysteresis. The accepted equilibrium transformation pressure of  $2.0 \pm 0.3$  GPa was estimated from measurements of samples under shear stress because the shear reduces the hysteresis;<sup>1</sup> measurements without applied shear give the pressure of the onset of the transformation between 2.9 (Ref. 9) and 9.0 GPa.<sup>10</sup> Impurities also strongly affect the onset pressure.<sup>1</sup> We know of no experimental data that explores the low-temperature regime; higher temperatures have been examined only indirectly using shockwave experiments.<sup>11-14</sup>

It is possible to use first-principles methods to calculate the zero-temperature internal energy  $\Phi_0(V)$  as well as the free-energy contributions from the ions,  $F_I(T, V)$ , and the electrons,  $F_E(T, V)$ , to give the complete equation of state

$$F(T, V) = \Phi_0(V) + F_I(T, V) + F_E(T, V). \quad (1)$$

Because of the large computational effort required to calculate the free energy of Eq. (1) over a significant range of volumes and temperatures, we have chosen to use a tight-binding model instead of conventional first-principles electronic-structure methods. The functional fitting forms are those developed at the U.S. Naval Research Laboratory.<sup>15-17</sup>

The model's accurate emulation of first-principles calculations (in this case the WIEN97 code<sup>18</sup>) requires optimization of a single tight-binding parametrization such that the model closely reproduces the relative total energies of selected crystal structures. The structures are chosen to be both simple and representative: simple enough to make the first-principles calculations feasible and representative of all microscopic environments the model is aimed at describing. A comparison of total energies as a function of volume with structures fulfilling these requirements is shown in Fig. 1. Not shown but included in the fit as independent structures are fcc crystals distorted to correspond to the longitudinal and transverse phonons at the reciprocal-space high-symmetry point  $X$ . These additional structures fine-tune the model's ability to correctly describe lattice vibrations.<sup>19</sup> Crucial for convergence of the fitting procedure is to fit the cubic-structure energy bands at high-symmetry points in reciprocal space.<sup>20,21</sup>

The electronic contribution to the free energy depends on the electronic density of states (DOS) as a function of volume,  $n(E, V)$ . The occupation of these states, given by the Fermi distribution  $f(E, T) = [e^{(E-E_f)/(k_B T)} + 1]^{-1}$ , determines their entropy<sup>22</sup>

$$S_{el}(T, V) = -k_B \int [f \ln f + (1-f) \ln(1-f)] n(E, V) dE, \quad (2)$$

and hence the electronic contribution to the free energy  $F_E(T, V) = -TS_{el}(T, V)$ . This contribution is small compared to that of the ions but is included for completeness.

The ionic contribution to the free energy depends on the phonon DOS,  $g(\omega, V)$ , through the zero-point energy

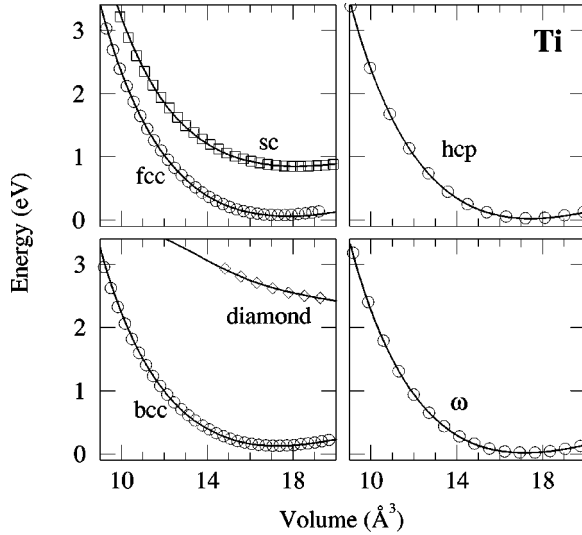


FIG. 1. Calculated energies for the crystal structures in the fitting database. Symbols are the first-principles results and solid lines are calculated from the fitted tight-binding model. Also included in the fit (but not shown here) is the fcc crystal with distortions corresponding to the longitudinal and transverse phonons at the reciprocal-space high-symmetry point  $X$ . The  $\omega$  structure lies lowest in energy, in contrast to the experimentally found ground state, hcp.

$$U_{zero}(V) = \frac{1}{2} \int_{\Omega} \hbar \omega g(\omega, V) d\omega, \quad (3)$$

as well as the temperature-dependent, quasiharmonic free energy<sup>22</sup>

$$F_H(T, V) = k_B T \int_{\Omega} \ln[1 - e^{-\hbar \omega / k_B T}] g(\omega, V) d\omega. \quad (4)$$

This differs from the volume-independent harmonic approximation in that the quasiharmonic approximation uses phonons calculated for small atomic displacements (i.e., harmonic) around the atomic positions for each crystal structure and volume. The resulting phonon frequencies are therefore volume dependent, which implicitly includes some anharmonic contributions neglected in a purely harmonic theory, but certainly misses other high-temperature anharmonic contributions. The theory should be most accurate at low temperatures and should lose accuracy as one approaches the melting temperature. Moreover, thermodynamics in this approximation are only possible when the quasiharmonic phonons for any given crystal structure and volume are stable, which may not be true if that crystal can lower its total energy by spontaneously and continuously distorting into another crystal structure. At elevated temperatures (near melting) this approximation also neglects some important anharmonic contributions to the free energy that can be responsible for stabilizing some of the high-temperature phases.

We have used the tight-binding model to calculate the electronic and the phonon DOS by evaluating the relevant energy eigenvalues and dynamical matrices on a fine mesh of wave vectors in the first Brillouin zone. In both cases the

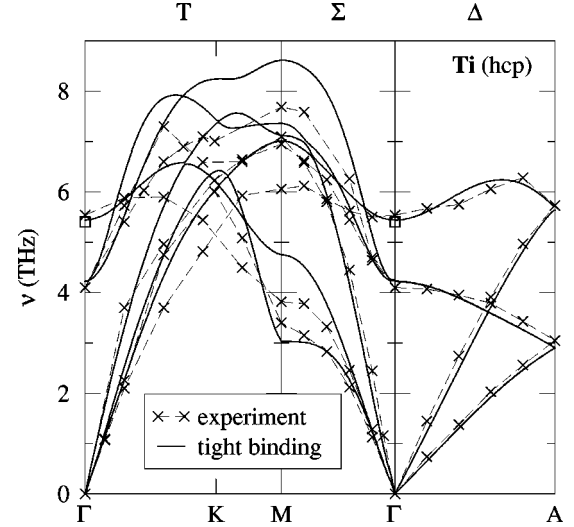


FIG. 2. Experimental (crosses) (Ref. 27) and tight-binding (solid lines) phonon dispersion of titanium in the hcp crystal structure at ambient pressure. Although some experimental details are not reproduced by our tight-binding model, the overall agreement is quite good. The diamond at  $\Gamma$  is from a first-principles frozen-phonon calculation.

spectrum is smeared with a Gaussian, chosen to be as small as possible while keeping the DOS smooth and continuous. The mesh is refined until the free energy converges.

The dynamical matrix at a given wave vector  $\mathbf{q}$  is the Fourier transform of the force constants, which we calculate from the tight-binding model by the direct-force method.<sup>23–26</sup> This method requires large simulation cells consisting of repeated unit cells transposed by vectors  $\ell$ ; the forces on all atoms are calculated in response to the displacement of the atom(s) in one unit cell. Our simulation cells contain 128 (hcp), 81 ( $\omega$ ), and 128 atoms (bcc); for more details we refer the reader to Ref. 19.

Figure 2 compares our calculated phonon dispersion for the hcp structure to experimental data.<sup>27</sup> The overall agreement is good, in particular near the zone center (around  $\Gamma$ ) and along the vertical direction (parallel to the  $c$  axis). Frequencies of modes in horizontal directions (perpendicular to the  $c$  axis) away from the zone center are somewhat high compared to experiment. Another experimental measurement of the phonon dispersion<sup>28</sup> shows similar agreement. The main characteristics, which the tight-binding model captures, give a reliable DOS (see Fig. 5 of Ref. 27), the relevant entity used in Eqs. (3) and (4) to calculate the phonon contribution to the free energy. The phonon dispersion we predict for the  $\omega$  crystal structure is shown in Fig. 3.

Figure 4 shows the calculated phonon DOS for the hcp crystal structure. Some differences between the calculations with 54 and 128 atoms are visible but change the calculated free energies, which integrate over the DOS, by less than 0.1%; our final result, the phase transformation line (see below), is not noticeably affected.

The phonon density of states is calculated for the hcp,<sup>33</sup>  $\omega$ , and bcc structures at a dozen volumes corresponding to pressures in the range from 0 to 170 GPa and is then used to evaluate the Gibbs free energy,<sup>22</sup>  $G(T, P) = F(T, V) + PV$ .

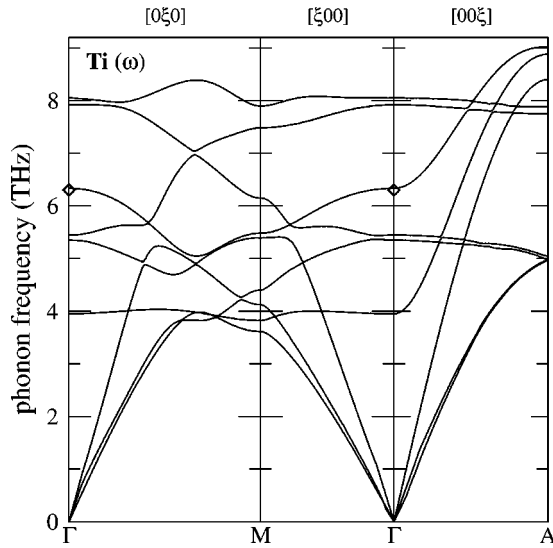


FIG. 3. Predicted tight-binding phonon dispersion of titanium in the  $\omega$  crystal structure at ambient pressure. Symmetry dictates that some phonon energies be degenerate at high-symmetry points, e.g., at  $\Gamma$  (000); slight numerical errors in the calculated forces destroy these degeneracies. The diamond at  $\Gamma$  is from a first-principles frozen-phonon calculation.

Comparison of the Gibbs free energies as a function of pressure and temperature for the hcp and  $\omega$  crystal structures allows us to identify the phase transformation line. This approach is extremely demanding because tiny errors in the relative free energies can dramatically alter the phase boundary. Figure 5 shows good agreement of our theoretically calculated  $\alpha \rightarrow \omega$  phase transformation line with the experimental phase diagram.<sup>29</sup> The calculated transition temperature at zero pressure is  $\approx 280$  K.

At normal pressure we know of no experimental data that show that the  $\omega$  phase is the correct zero-temperature ground state, nor are we aware of any experimental data indicating the opposite. It has recently been shown that energy barriers exist for this phase transformation<sup>30</sup> that may make it extremely difficult to verify at low temperatures. Thus the ki-

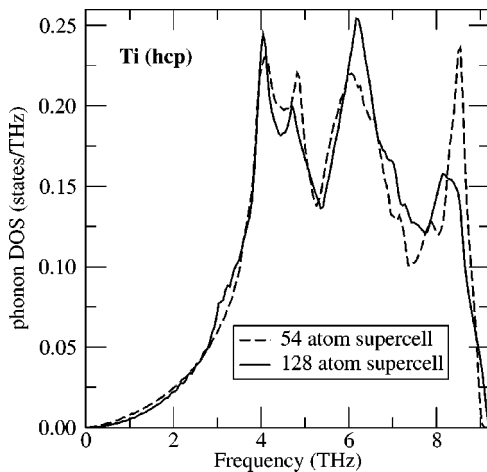


FIG. 4. The phonon DOS for hcp Ti calculated using supercells with 54 and 128 atoms.

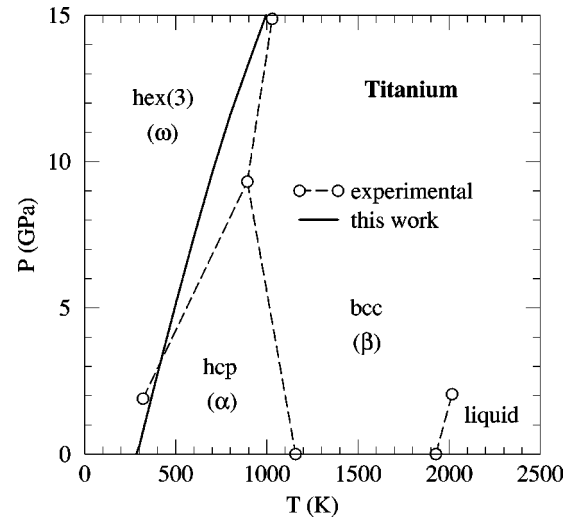


FIG. 5. The phase diagram of titanium. The dashed lines connect the experimental data points given by Young (Ref. 29); the solid line shows our calculated  $\alpha \rightarrow \omega$  transformation. Thermal stabilization explains why at room temperature the experimentally observed hcp structure is favored over the  $\omega$  structure (the calculated static-lattice ground state).

netics may be just too sluggish for the system to bring itself into true thermodynamic equilibrium.

We were not able to similarly calculate and include in Fig. 5 the transition into the bcc structure. The open bcc structure appears to be dynamically stabilized by entropy and anharmonic effects. Some quasiharmonic phonon modes are unstable due to a spontaneous instability of the bcc crystal structure into the  $\omega$  phase. There is no energy barrier to this continuous transformation. In particular, this causes the lon-

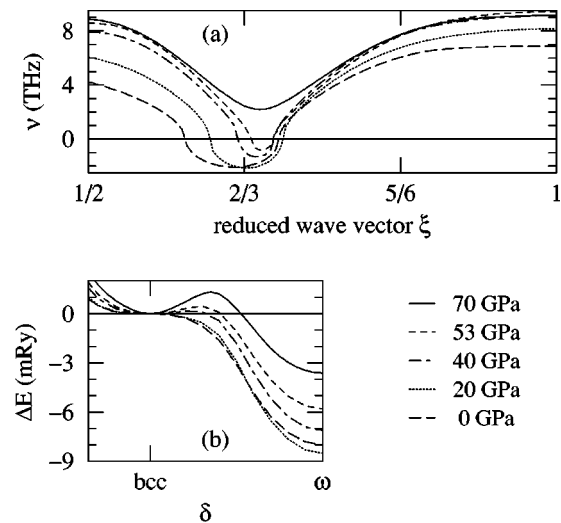


FIG. 6. (a) Calculated quasiharmonic frequencies of longitudinal phonon modes around the wave vector  $\mathbf{q} = \frac{2}{3}(1,1,1)$ , which distorts the bcc crystal into the  $\omega$  phase. (b) Calculated energy landscape for the bcc to  $\omega$  pathway. The negative phonon frequencies shown in (a) are  $i\sqrt{\nu^2}$  when  $\nu^2$  is negative. These frequencies thus represent the imaginary part of the phonon frequency for unstable modes.

gitudinal phonon mode with wave vector  $\mathbf{q}=\frac{2}{3}(1,1,1)$ , which distorts the bcc crystal into the  $\omega$  phase, to be unstable below pressures of roughly 40 GPa. The mechanical instability of this phonon mode at low temperatures is also seen experimentally; the martensitic phase transition from the bcc phase to the hcp phase prevents the high-temperature bcc phase from being quenched to room temperature.<sup>31</sup> One branch of transverse phonon modes with wave vectors  $(\xi, \xi, 0)$ , which are related to the bcc to hcp transition, also appears unstable in our treatment. Both of these instabilities are consistent with strictly first-principles calculations of phonons.<sup>32</sup>

Figure 6(a) shows the relevant segment of the  $(\xi, \xi, \xi)$  branch. The energy of the corresponding pathway from the bcc phase to the  $\omega$  phase, shown in Fig. 6(b), develops local minima for the bcc phase at pressures of roughly 40 GPa, but at lower pressures the crystal can deform from bcc to  $\omega$  without encountering an energy barrier. This pathway can be viewed as planes moving in accordance with the wave vector  $\mathbf{q}=\frac{2}{3}(1,1,1)$  or as chains of atoms along the body diagonal

moving with respect to each other. Calculations of the energy needed to move such a single chain of atoms indicate that for small displacements the movement is energetically favored, whereas the movement of a single atom is not.

In conclusion, we have used a completely theoretical approach, without any experimental input, to calculate the Gibbs free energies of competing crystal phases in titanium. Comparison of the hcp and  $\omega$  Gibbs free energies results in a pressure and temperature dependence of the structural phase transition in good agreement with experiment and serves to explain how finite-temperature entropy effects stabilize the experimentally found room-temperature hcp crystal structure over the theoretically found static-lattice  $\omega$ -phase ground state. For the  $\omega$  structure the phonon dispersion is predicted.

We thank Matthias Graf, Carl Greeff, Dallas Trinkle, and Duane Wallace for helpful and encouraging discussions. This research was supported by the U.S. Department of Energy under Contract No. W-7405-ENG-36. All FLAPW calculations were performed using the WIEN97 package.<sup>18</sup>

- 
- <sup>1</sup>S.K. Sikka, Y.K. Vohra, and R. Chidambaram, *Prog. Mater. Sci.* **27**, 245 (1982).
- <sup>2</sup>J.S. Gyanchandani, S.C. Gupta, S.K. Sikka, and R. Chidambaram, *J. Phys.: Condens. Matter* **2**, 301 (1990).
- <sup>3</sup>R. Ahuja, J.M. Wills, B. Johansson, and O. Eriksson, *Phys. Rev. B* **48**, 16 269 (1993).
- <sup>4</sup>G. Jomard, L. Magaud, and A. Pasturel, *Philos. Mag. B* **77**, 67 (1998).
- <sup>5</sup>C.W. Greeff, D.R. Trinkle, and R.C. Albers, *J. Appl. Phys.* **90**, 2221 (2001).
- <sup>6</sup>M.J. Mehl and D.A. Papaconstantopoulos, *Europhys. Lett.* **60**, 248 (2002).
- <sup>7</sup>Y.K. Vohra and P.T. Spencer, *Phys. Rev. Lett.* **86**, 3068 (2001).
- <sup>8</sup>Y. Akahama, H. Kawamura, and T.L. Bihan, *Phys. Rev. Lett.* **87**, 275503 (2001).
- <sup>9</sup>Y.K. Vohra, S.K. Sikka, S.N. Vaidya, and R. Chidambaram, *J. Phys. Chem. Solids* **38**, 1293 (1977).
- <sup>10</sup>F. P. Bundy, General Electric Research Laboratory Report No. 63-rl-3481 c, 1963.
- <sup>11</sup>R. G. McQueen, S. P. Marsh, J. W. Taylor, J. N. Fritz, and W. J. Carter, *High Velocity Impact Phenomena* (Academic, New York, 1970).
- <sup>12</sup>A.R. Kutsar, M.N. Pavlovskii, and V.V. Komissarov, *Pis'ma Zh. Eksp. Teor. Fiz.* **35**, 91 (1982) [*JETP Lett.* **35**, 108 (1982)].
- <sup>13</sup>G. T. Gray, C. E. Morris, and A. C. Lawson, *Titanium '92 Science and Technology* (Minerals, Metals, and Materials Society, Warrendale, PA, 1993).
- <sup>14</sup>R.F. Trunin, G.V. Simakov, and A.B. Medvedev, *High Temp.* **37**, 851 (1999).
- <sup>15</sup>R.E. Cohen, M.J. Mehl, and D.A. Papaconstantopoulos, *Phys. Rev. B* **50**, 14 694 (1994).
- <sup>16</sup>M.J. Mehl and D.A. Papaconstantopoulos, *Phys. Rev. B* **54**, 4519 (1996).
- <sup>17</sup>S.H. Yang, M.J. Mehl, and D.A. Papaconstantopoulos, *Phys. Rev. B* **57**, R2013 (1998).
- <sup>18</sup>P. Blaha, K. Schwarz, and J. Luitz, computer code WIEN97, (Techn. Universitat, Wien, Austria, 1999).
- <sup>19</sup>S.P. Rudin, M.D. Jones, C.W. Greeff, and R.C. Albers, *Phys. Rev. B* **65**, 235114 (2002).
- <sup>20</sup>M.D. Jones and R.C. Albers, *Phys. Rev. B* **66**, 134105 (2002).
- <sup>21</sup>D. A. Papaconstantopoulos, *Handbook of the Band Structure of Elemental Solids* (Plenum, New York, 1986).
- <sup>22</sup>R. K. Pathria, *Statistical Mechanics* (Pergamon, Oxford, 1972).
- <sup>23</sup>K. Kunc and R.M. Martin, *Phys. Rev. Lett.* **48**, 406 (1982).
- <sup>24</sup>S. Wei and M.Y. Chou, *Phys. Rev. Lett.* **69**, 2799 (1992).
- <sup>25</sup>W. Frank, C. Elsasser, and M. Fahnle, *Phys. Rev. Lett.* **74**, 1791 (1995).
- <sup>26</sup>K. Parlinski, Z.Q. Li, and Y. Kawazoe, *Phys. Rev. Lett.* **78**, 4063 (1997).
- <sup>27</sup>C. Stassis, D. Arch, B.N. Harmon, and N. Wakabayashi, *Phys. Rev. B* **19**, 181 (1979).
- <sup>28</sup>N. Wakabayashi, R.H. Scherm, and H.G. Smith, *Phys. Rev. B* **25**, 5122 (1982).
- <sup>29</sup>D. A. Young, *Phase Diagrams of the Elements* (University of California Press, Berkeley, 1991).
- <sup>30</sup>D.R. Trinkle, R.G. Hennig, S.G. Srinivasan, M.D.J.D.M. Hatch, H.T. Stokes, R.C. Albers, and J.W. Wilkins, *Phys. Rev. Lett.* **91**, 025701 (2003).
- <sup>31</sup>W. Petry, A. Heiming, J. Trampenau, M. Alba, C. Herzig, H.R. Schober, and G. Vogl, *Phys. Rev. B* **43**, 10 933 (1991).
- <sup>32</sup>K. Persson, M. Ekman, and V. Ozolins, *Phys. Rev. B* **61**, 11 221 (2000).
- <sup>33</sup>The  $c$  over  $a$  ratio of the hcp structure is varied to give the lowest static-lattice energy, i.e., in particular, at high pressures the calculation is done for a hexagonal crystal with a  $c/a$  larger than the ideal value.